



Liquid petroleum gas sensor based on SnO₂/Pd composite films deposited on Si/SiO₂ substrates

S. Majumder, S. Hussain, R. Bhar, A.K. Pal*

Department of Instrumentation Science, USIC Building, Jadavpur University, Calcutta-700 032, India

Received 4 October 2006; received in revised form 15 December 2006; accepted 18 December 2006

Abstract

SnO₂/Pd composite films were synthesized by d.c. sputtering of a SnO₂ target followed by thermal evaporation of a thin layer of Pd on top of it. This structure, deposited on Si wafer with 300 μm SiO₂ on the top, was subjected to rapid thermal annealing at 573 K for 5 min for the incorporation of Pd in SnO₂. The films were characterized by microstructural, optical, FTIR and Raman studies. Liquid petroleum gas (LPG) sensing measurements were carried out on these films. Sensitivity of 72% was obtained at an operating temperature of ~573 K. The response time for these sensors was found to be ~27 s. Sensitivity was found to increase with grain growth at higher sensing temperatures. It could be observed that the selectivity for LPG is extremely good as compared to that of methane, hydrogen, CO₂ and C₂H₅OH.

© 2007 Elsevier Ltd. All rights reserved.

Keywords: Sensor; Sputtering

1. Introduction

Gas sensors are in high demand for industrial, medicinal, commercial and domestic applications. Generally, these sensors using oxide semiconductor thin films as sensing elements are very promising due to their relative ease of fabrication, low production cost, high yield, ability to sense in hostile environment and compatibility with micromachining technology [1–4]. Different dopants were utilized to enhance the sensitivity and selectivity of these oxide materials. The surface chemistry of the sensor films gets modified due to creation of oxygen vacancies which act as donors to increase the film conductance. Addition of dopants was found to modify the optical and electrical properties significantly and this property has been utilized to realize gas sensors with faster response and greater selectivity towards a given gas.

Among various metal oxide gas sensors, SnO₂ has emerged as a potential material in recent years [5–8] and a number of techniques such as chemical vapour deposition (CVD) [9], physical vapour deposition, sputtering [10],

thermal evaporation [11], e-beam evaporation [12], spray pyrolysis [13], sol gel [14], etc., have been utilized to deposit SnO₂ on glass or alumina substrates. Considering the commercial aspects of the sensors as regards to the large-scale manufacturing at low cost, one has to opt for micro electro-mechanical system (MEMS) technology that would require SnO₂ to be deposited onto Si substrate with a native oxide layer on it (Si/SiO₂) so that one may obtain large number of sensor chips with micro-heaters attached to it by utilizing photolithography technique. There are not many studies reported so far on SnO₂ films deposited onto Si/SiO₂ substrates for realizing LPG sensors.

The present study deals with the deposition of SnO₂ films onto Si/SiO₂ substrates by d.c. sputtering of a SnO₂ target. Pd was incorporated by depositing a layer of Pd over the SnO₂ film by thermal evaporation followed by rapid thermal annealing of the bilayer structure (Pd/SnO₂) obtained as above for dispersing Pd in SnO₂. Generally, the microstructure and hence the physical properties, depend critically on the substrate and other deposition parameters. The resultant films were characterized by microstructural, optical, FTIR and Raman studies. Liquid petroleum gas (LPG) sensing measurements were carried out in these films.

*Corresponding author.

E-mail address: msakp2002@yahoo.co.in (A.K. Pal).

2. Experimental

A conventional d.c. sputtering unit, which could be pumped down to $\sim 10^{-4}$ Pa, was used to sputter a 10 cm diameter SnO₂ target for the deposition of SnO₂ film on Si/SiO₂ substrate. SiO₂ layer of ~ 300 μm thickness was incorporated on a silicon wafer (100) of diameter ~ 7.5 cm by thermal oxidation in a quartz diffusion furnace in which oxygen could be introduced in a controlled manner. The target was sputtered in Ar+O₂ plasma at ~ 1 kV and 1.3 mA/cm². Relative amount of oxygen was varied to regulate the sheet resistance of the SnO₂ films deposited. The thickness of the films so obtained was in the range of 1.5–2 μm. The deposition was carried out at room temperature but it was observed that the substrate temperature rose to ~ 323 K after 90 min of continuous sputtering. Pd was thermally evaporated on the as-deposited SnO₂ film using an alumina-coated tantalum boat. The rate of Pd evaporation was ~ 0.15 nm/s as measured by a quartz crystal oscillator. This layer of Pd was dispersed in SnO₂ by subjecting the bilayer structure of Pd/SnO₂ deposited on Si/SiO₂ substrates to rapid thermal annealing (RTA) at different thermal budgets. The temperature ramp used here was 5 °C/s. Optimum thickness of Pd for obtaining best sensitivity was determined by measuring the sensitivity of the composite films containing different amount of Pd on it.

Small pieces of dimension ~ 0.5 cm \times 0.5 cm of the films were used for sensitivity measurement. Electrical contacts were made at the end of these sensor elements by evaporating appropriate aluminium pads. A multimeter (Hewlett Packard 34401A) and a constant voltage source (Advantest T6142) were used to monitor the changes in the resistance of the film with exposure to different concentrations of LPG. Commercially available LPG gas was taken in measured amounts in an ampoule which could be diluted with argon gas to get the required concentration of LPG (in ppm) before introducing the same in the test chamber. The sensitivity (*S*) of the sensors was measured as the change in the sample resistance in presence of test gas with respect to its resistance in air at the same temperature such that *S* may be expressed as: $S = [(R_{\text{air}} - R_{\text{gas}}) / R_{\text{air}}] \times 100$; where *R*_{air} and *R*_{gas} denotes the resistances of the sensors in air and in the test gas, respectively.

Scanning electron microscopy (SEM) and X-ray diffraction (XRD) using Cu K_α line (0.154 nm) were used to obtain the microstructural information. Optical studies were performed by measuring transmittance and absorbance in the wavelength region $\lambda = 200$ –900 nm at room temperature using a spectrophotometer (Hitachi-U3410). The spectra were recorded with a resolution of $\lambda \sim 0.07$ nm along with a photometric accuracy of $\pm 0.3\%$ for transmittance measurements. Raman spectra were recorded using Renishaw inVia micro-Raman spectrometer using 514 nm Argon laser. FTIR spectra were recorded in the range of 4000–400 cm⁻¹ by using a Nicolet™-380 FTIR.

3. Results and discussion

SnO₂ films having nominal thickness ~ 1.8 μm were deposited onto Si/SiO₂ substrate. Incorporation of Pd in the SnO₂ layer was carried out by subjecting the Pd/SnO₂ bilayer to rapid thermal annealing at different thermal budget (temperature \times time). The amount of palladium was varied by changing the thickness of the evaporated Pd layer to ascertain the critical amount of Pd that has to be incorporated in SnO₂ matrix for obtaining highest sensitivity. It was found from the XRD studies and gas sensitivity measurements on the above samples that there existed a critical thermal budget of RTA for the dispersion of Pd and also an optimum amount of Pd to be incorporated in SnO₂ layer that would give the highest sensitivity. These will be apparent from the following observations.

3.1. Microstructural studies

Fig. 1(a) shows the XRD spectrum of a representative as-deposited SnO₂ film which shows peaks of SnO₂ for reflections from (1 1 0), (1 0 1) and (2 1 1) planes. The peaks are broad and the most intense peak is due to the reflections from (1 0 1) planes. The intensities of the other peaks are lower than that for the (1 0 1) planes indicating polycrystalline nature of the as-deposited films. SEM picture of the same film (Fig. 2(a)) shows a smooth surface and the film to be a compact one. The texture of the SnO₂ film with Pd (~ 7 nm) on top did not indicate any significant change (Fig. 2(b)) from that of the as-deposited SnO₂ film while the XRD pattern of the same film (Fig. 1(b)) indicated an additional reflection of Pd from (1 1 1) plane besides the ones observed for as-deposited SnO₂ film. It may be observed here that the intensity of peaks for reflections from (1 1 0), (1 0 1) and (2 1 1) planes of SnO₂ became weaker in films with Pd on it. The morphology of the above Pd incorporated SnO₂ films changed with rapid thermal annealing and grain growth was observed from the SEM picture of the film which was subjected to rapid thermal annealing at 573 K for 5 min (Fig. 2(e)). The XRD spectra of this annealed film showed (Fig. 1(c)) two peaks corresponding to reflections from (1 0 1) and (2 1 1) plane of SnO₂ along with that for (1 1 1) planes of Pd. It is interesting to observe that the intensities of the peaks for SnO₂ diminished significantly and the peak for (1 1 0) planes vanished. When this film was exposed to LPG (3000 ppm) for sensitivity measurements at temperature of 473 K, the peak for reflections from (1 1 0) plane of SnO₂ reappeared and the intensity of the peak for Pd significantly diminished (Fig. 1(d)). Fig. 2(f) shows the corresponding SEM micrograph of the film. One could observe distinct grain growth when exposed to LPG at higher temperature. It may be mentioned here that during sensitivity test, the films get further annealed at temperature used during sensitivity measurement. Some small voids amidst the film structure appeared which would provide

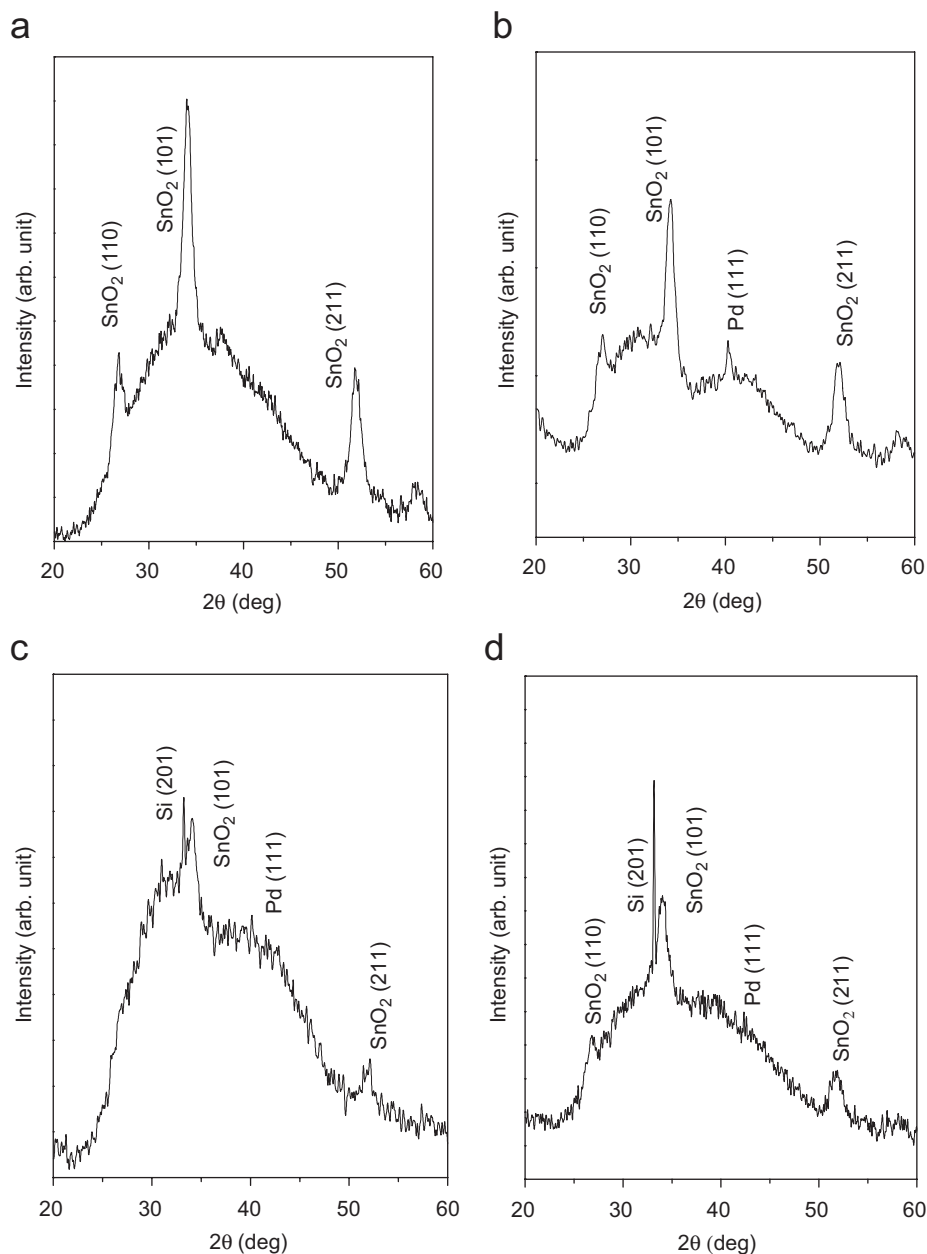


Fig. 1. XRD spectra for some representative films: (a) as-deposited SnO_2 film; (b) Pd/SnO_2 film and (c) Pd/SnO_2 film after RTP at 573 K for 5 min while (d) represents the XRD for (c) when exposed to LPG at 3000 ppm at 473 K.

larger surface area for the interaction of the gas molecules and the films. It may be noted here that with further increase in annealing temperature no significant grain growth was observed and the films developed cracks when annealed beyond 600 K.

The effect of annealing temperature and related dispersion of Pd in SnO_2 matrix will be apparent from the XRD spectra as shown in Fig. 3. The XRD spectrum of the as-deposited Pd/SnO_2 multilayer film is shown in Fig. 1(b). The above film was then subjected to RTA at different temperatures keeping the time fixed at 5 min. When the above film was subjected to RTA at 423 K, one may observe that Pd tends to diffuse in the SnO_2 matrix which is evident

from the decrease in Pd peak (Fig. 3(a)) and the corresponding micrograph (Fig. 2(c)) indicated grain growth. With increasing annealing temperature, one may observe gradual reduction in the intensity of Pd peak accompanied by broadening of the SnO_2 peaks till 573 K (Fig. 3(b)–(e)), beyond which the peaks for Pd as well as that for SnO_2 started regaining intensity (Fig. 3(e)). This would indicate precipitation of Pd at the surface through the grain boundaries of SnO_2 . Thus, one would expect complete dispersion of Pd in SnO_2 matrix by RTA with an annealing temperature of ~ 573 K and a duration of 5 min. One may also observe gradual grain growth (Fig. 2(c)–(e)) as the annealing temperature was increased from 423 to 573 K.

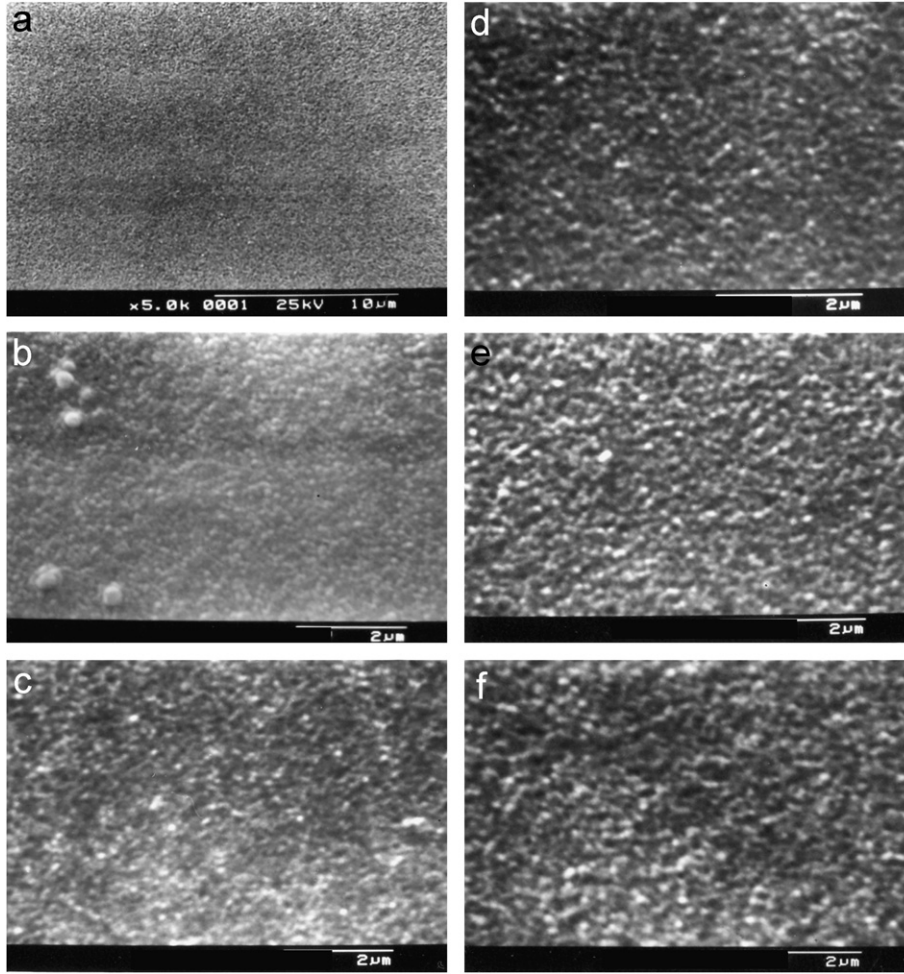


Fig. 2. SEM micrograph of some representative films (a) as-deposited SnO₂ film; (b) Pd/SnO₂ film; (c) Pd/SnO₂ film after RTA at 423 K for 5 min; (d) after RTA at 523 K, (e) after RTA at 573 K and (f) for the same film as (e) after LPG exposure (3000 ppm) at 473 K.

3.2. Optical properties

The absorption coefficients (α) of the SnO₂ films studies here were determined by measuring transmittance and reflectance in these films [15,16]. In general, the absorption coefficient (α) may be written as a function of the incident photon energy ($h\nu$) so that [16–18]

$$\alpha h\nu = A(h\nu - E_g)^m, \quad (1)$$

where A is a constant which is different for different transitions indicated by the different values of m . Depending on the nature of transition, m can have values 0.5, 2, 1.5 and 3 for allowed direct, allowed indirect, forbidden direct and forbidden indirect transitions, respectively. Eq. (1) may be rewritten as

$$\ln(\alpha h\nu) = \ln A + m \ln(h\nu - E_g), \quad (2)$$

so that

$$\frac{d[\ln(\alpha h\nu)]}{d[h\nu]} = \frac{m}{h\nu - E_g}. \quad (3)$$

Eq. (3) suggests that a plot of $d[\ln(\alpha h\nu)]/d[h\nu]$ versus $h\nu$ (Fig. 4(a)) will indicate a divergence at $h\nu = E_g$ from which

an approximate value of E_g may be obtained. Once E_g is found, the value of m can easily be calculated (Eq. (2)) from the slope of the plot of $\ln(\alpha h\nu)$ versus $\ln(h\nu - E_g)$. Inset of Fig. 4(a) shows the plot of $\ln(\alpha h\nu)$ versus $\ln(h\nu - E_g)$ for a representative film, from which one may obtain the value of $m = 0.47$ which is nearly equal to 0.5. This would suggest direct transition occurring in this film. The band gap (E_g) for the films was determined by extrapolating the linear portion of the $(\alpha h\nu)^2$ versus $h\nu$ plot to $(\alpha h\nu)^2 = 0$. Such a plot for four representative films are shown in Fig. 4(a)–(d). The as-deposited films had higher band gap (~ 3.31 eV) (Fig. 4(a)) than those for Pd-incorporated films (~ 3.2 eV) (Fig. 4(b)). The fall of α for as-deposited SnO₂ film is sharper than that for Pd/SnO₂ film. This effect may be attributed to the dispersion of Pd particles in SnO₂ matrix. Band gap increased (~ 3.24 eV) when the Pd/SnO₂ film was subjected to RTA at 573 K (Fig. 4(c)) and upon exposure to LPG gas the fall in α became sharper as indicated in Fig. 4(d). One may also observe an increase of band gap of the Pd/SnO₂ film after exposure to LPG (Fig. 4(d)) which reaches near bulk band gap value of ~ 3.42 eV. This may be basically due to normal annealing for prolonged period at ~ 623 K while performing sensitivity tests leading to grain growth.

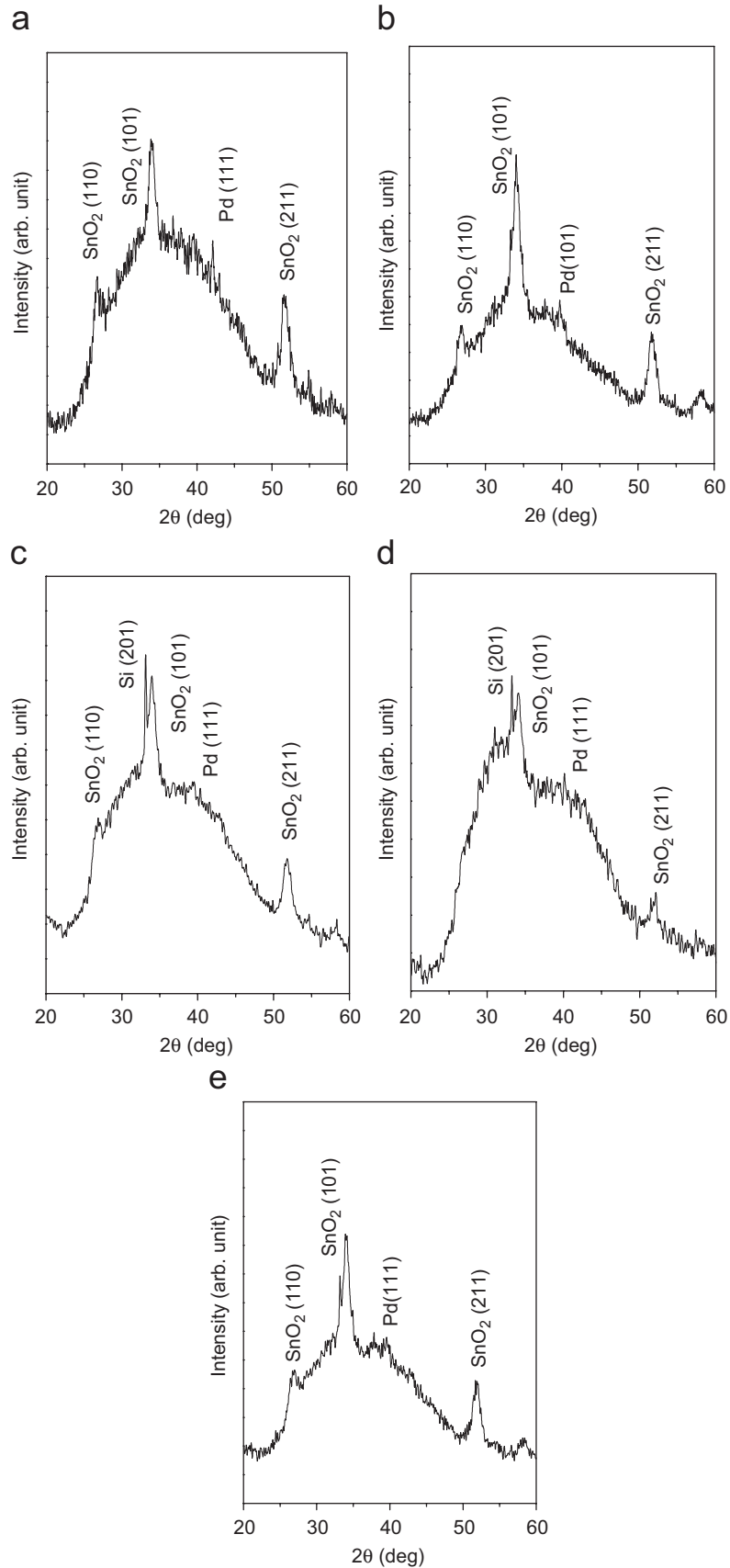


Fig. 3. XRD spectra for a representative Pd/SnO₂ film subjected to different RTA for 5 min at: (a) 423 K, (b) 473 K, (c) 523 K, (d) 573 K and (e) 623 K.

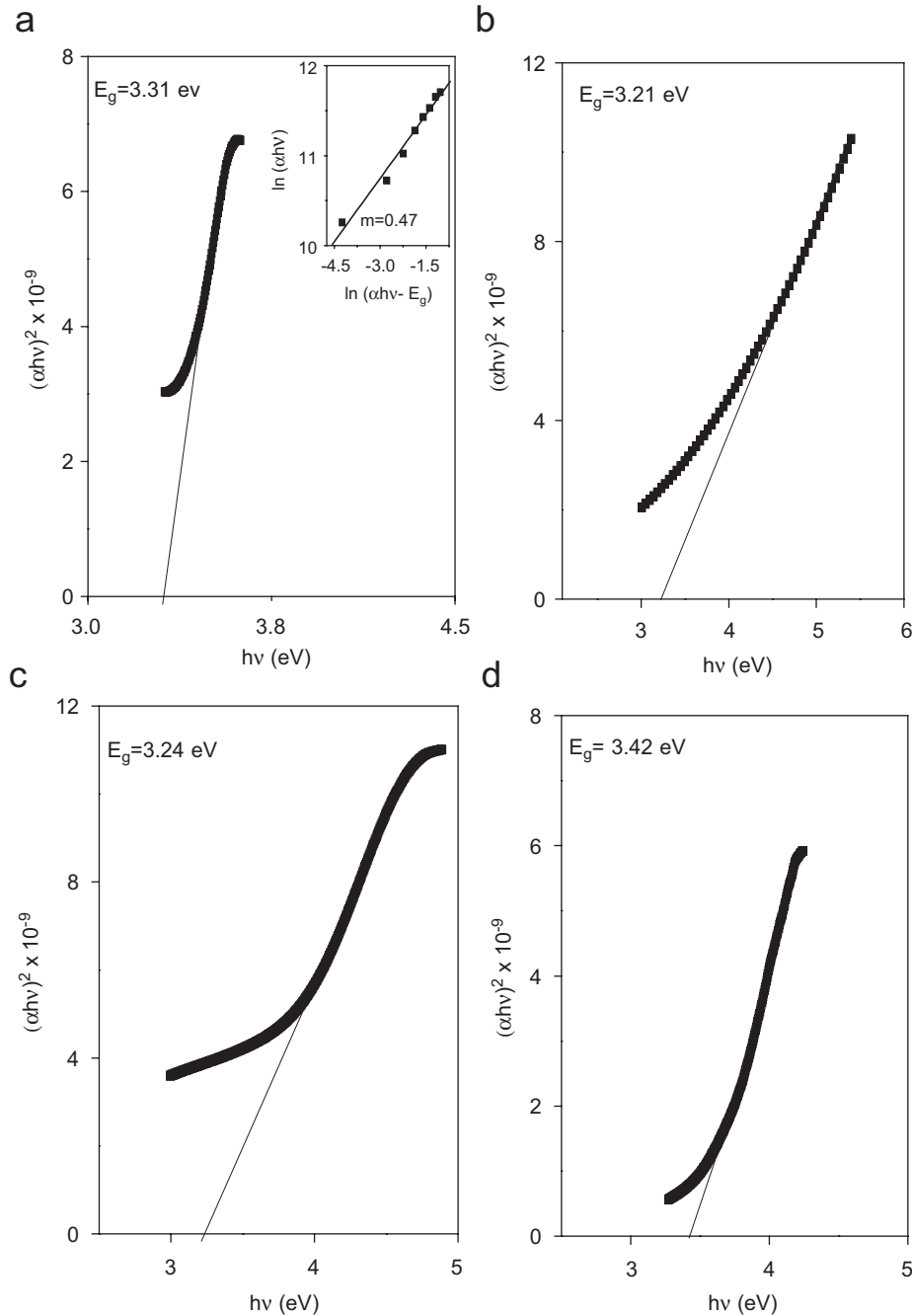


Fig. 4. Plot of $(\alpha hv)^2$ versus hv for representative films: (a) as-deposited SnO_2 film, (b) Pd/SnO_2 multilayer film; (c) same film as in (b) but subjected to RTA at 573 K for 5 min and (d) same film as in (c) but exposed to LPG with 3000 ppm.

3.3. Gas sensing properties

Aluminium contacts were deposited at the ends of the sensor films using appropriate mask by thermal evaporation. A heater was provided below the substrate holder to heat the sensor element and an electronic on/off controller controlled the temperature of the film. A thermocouple, placed on a dummy substrate beside the film, measured the sensor temperature. The whole assembly was placed inside

a test chamber in which LPG appropriately diluted with argon could be introduced.

The sensitivity test was carried out on the Pd/SnO_2 composite films deposited onto Si/SiO_2 substrates with different amount of Pd ranging from 2% to 10% and homogenized at identical RTA condition of 573 K for 5 min. These films were exposed to 3000 ppm of LPG in the test chamber. It may be observed (Fig. 5) that the sensitivity increased with increasing amount of Pd,

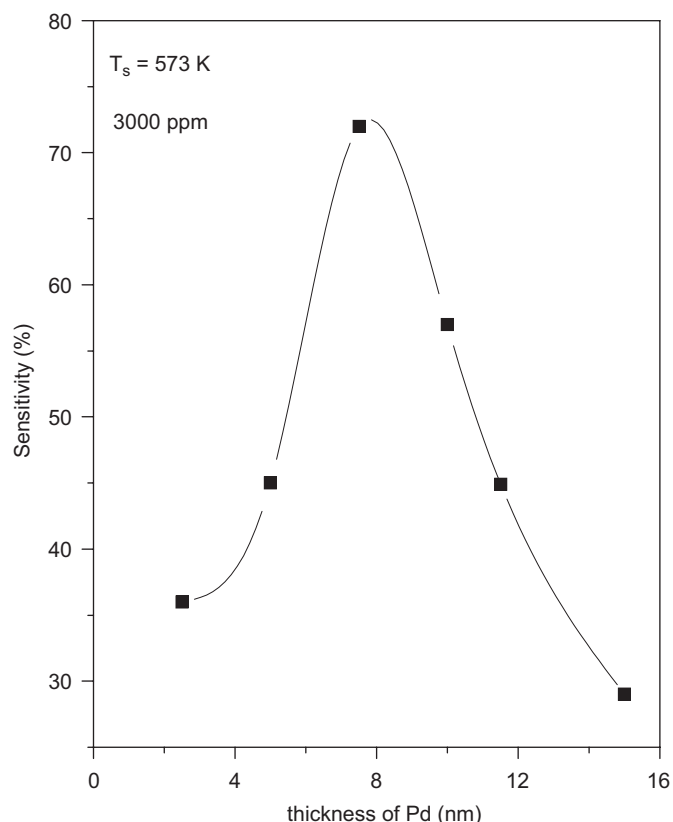


Fig. 5. Variation of sensitivity with LPG concentration at an operating temperature of 573 K for different amount of Pd in SnO₂ matrix.

reaching a maximum for films containing ~7 at% Pd, beyond which the sensitivity decreased sharply. Surface doping of SnO₂ layer by Pd was found to be a very effective method for improving the sensitivity of SnO₂ film [19]. It was interpreted by Korotcenkov et al. [19] that Pd surface additives on SnO₂ surface were basically of chemical nature. It may be noted here that thinner SnO₂ films (<1 μm) get poisoned after two/three exposure to LPG while for thicker (>2.5 μm) films, Pd incorporation by RTP seemed to be inadequate and as such the composite films did not indicate encouraging sensitivity. Thus, the optimum thickness of SnO₂ film used here was ~2 μm. The following discussions are based on the results obtained using SnO₂ films (~2 μm) containing 7 at% Pd.

The operating temperature is generally found to play an important role in determining sensitivity of the sensor. In general, there exists an optimum operating temperature for a sensor to achieve maximum sensitivity. For reliable operations of the sensor element, stabilization of sensor resistance at the operating temperature is essential. The optimum temperature depends on the sensing mechanism of the test gas and on the nature of the sensor surface at that particular temperature. It is known that propene, one of the common constituent gases in LPG, is more prone to hydrogenation at higher temperatures and presence of catalysts like Pd may induce catalytic activity even at room

temperature. Also, cracking of propane, the main constituent of LPG, to propene, may also be possible due to the presence of Pd leading to further hydrogenation activity in the films. Both the phenomena would culminate in an increase in conductivity of the SnO₂/Pd films when exposed to LPG at increasing temperature and the experimental observation (discussed below) are in conformity with the above.

The sensitivity and selectivity of a material may generally be controlled to some extent by selecting the temperature range of measurement. Depending on temperature, the binding between the different gas molecules and sensor surface would be modulated at a certain rate. The sensitivity of the Si/SiO₂/SnO₂/Pd structure synthesized as above was measured at various temperatures and concentrations by exposing it to LPG in measured proportion. Fig. 6 shows the variation of sensitivity with operating temperature of such samples when the LPG concentration was kept constant at ~3000 ppm. Curve-a of Fig. 6 was obtained when the same film was subjected to sensitivity tests with increasing temperature while curve-b was obtained by using fresh samples for sensitivity measurement at individual temperatures. It was observed

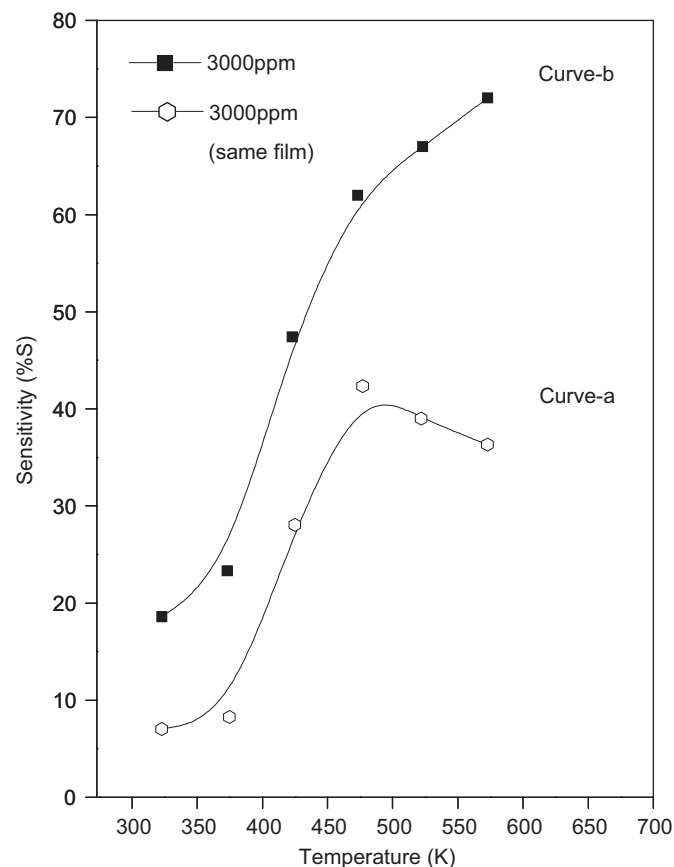


Fig. 6. Variation of sensitivity with temperature: curve-a shows the variation with fresh films for every temperature of measurements while curve-b shows the variation when the same film was used for the whole measurement.

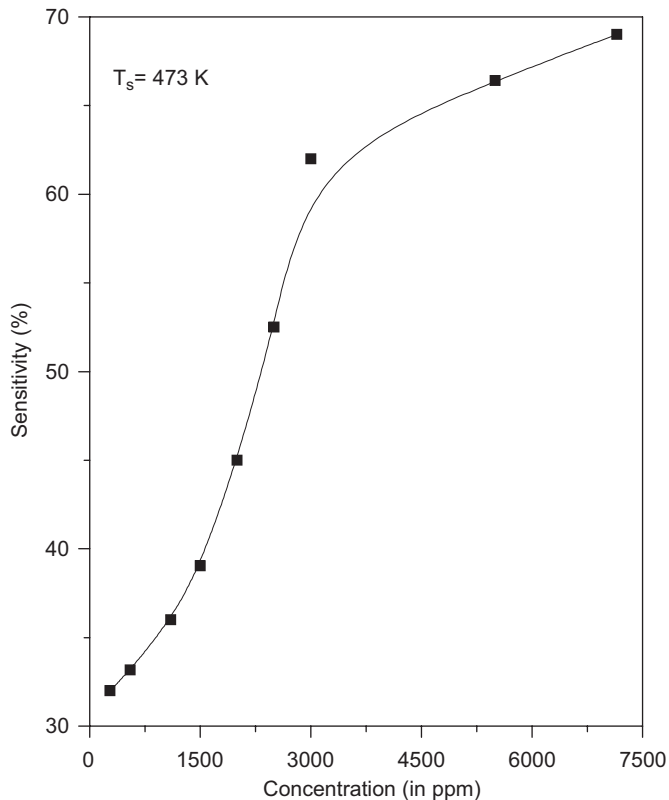


Fig. 7. Variation of sensitivity with LPG concentration at an operating temperature of 473 K.

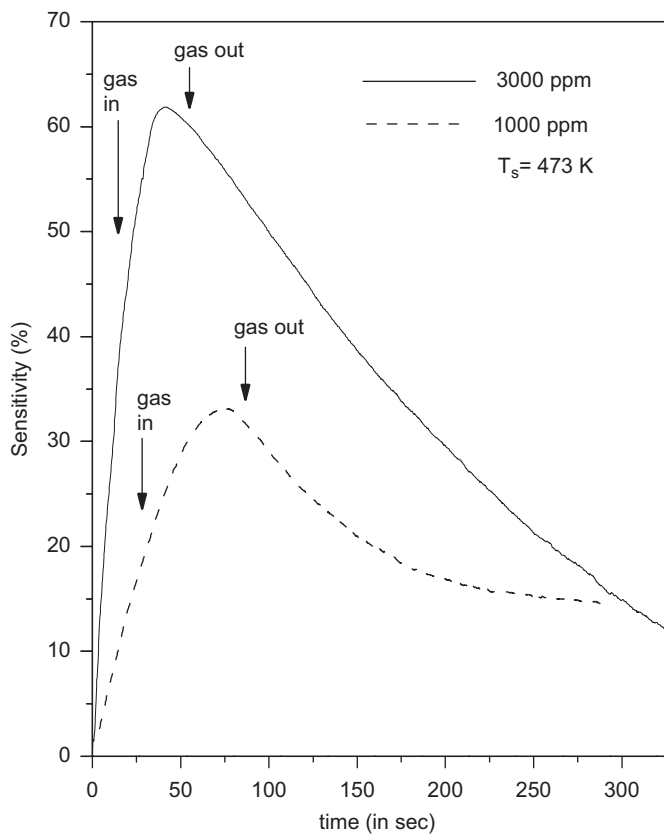


Fig. 8. Response characteristics of a representative Pd/SnO₂ film deposited onto Si/SiO₂ substrate.

that the sensitivity increased with increasing temperatures in both the cases. It was further observed that the sensitivity increased sharply after 373 K and reached a value of 72% at 573 K (curve-b). The variation of sensitivity with temperature was found to be nearly linear in the temperature range of 373–500 K. However, when the measurements were carried out on the same film at different temperatures, the sensitivity also increased with temperature but attained a maximum value of ~44% at 473 K (Fig. 6, curve-a). With further increase in temperature, the sensitivity was found to decrease. This may be attributed to the effect of multiple exposures of the film to the test gas when one would expect the reduction of active sites favouring hydrogenation activity after each exposure.

Fig. 7 shows the dependence of sensitivity on LPG concentration at an operating temperature of ~473 K. As the concentration of LPG increased, the sensitivity was found to increase sharply till 3000 ppm beyond which it showed a gradual increase with further increase in LPG concentration. This trend persisted till 4000 ppm, beyond which it tended to saturate. It seems that due to increase in LPG concentration more gas molecules would be available to react with the oxygen anions. Thus, one would expect the sensitivity response to increase with the increase in LPG concentration as observed here and this would tend to saturate with increase in LPG concentration since there

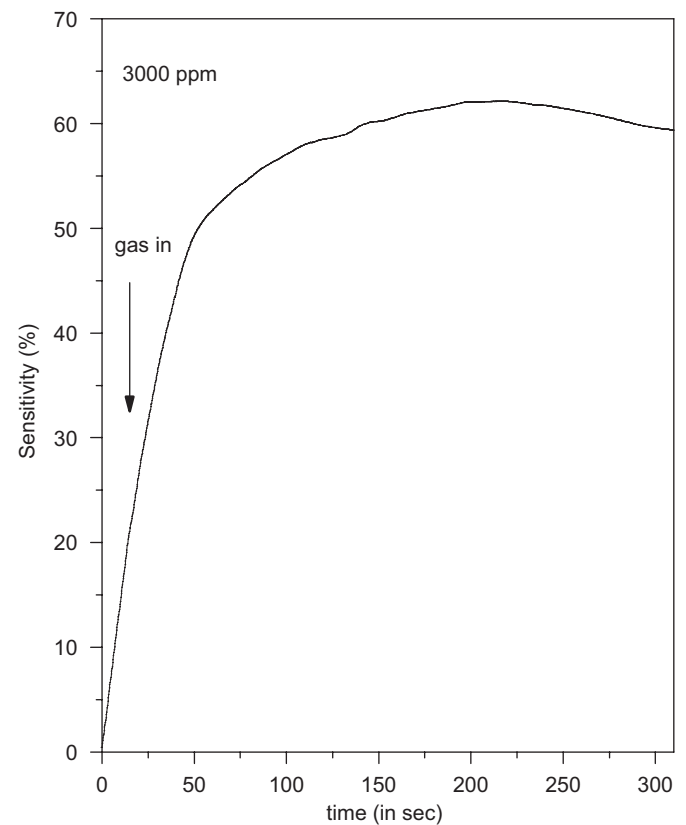


Fig. 9. Variation of sensitivity with time when exposed to LPG at 3000 ppm.

would not be sufficient number of oxygen anions available to contribute to the detecting mechanism.

The response characteristics of the palladium-incorporated SnO₂ films deposited onto Si/SiO₂ when exposed to two different concentrations of LPG (3000 and 1000 ppm) are presented in Fig. 8. All the measurements were carried out at an operating temperature of 473 K. It may be observed here that the films attain the maximum sensitivity in ~30 s for both the concentration level of LPG. When the test gas was removed, the sensitivity tended to come back nearly to its initial state in an exponential manner. The response time is defined as the time taken for the sensor to reach 90% of the saturation value in presence of the test gas. The response time for LPG gas was found to be ~27 s.

Fig. 9 depicts the variation of sensitivity with time as the test gas with a concentration of 3000 ppm is introduced

inside the chamber. The sensitivity gradually increased with time, reached the maximum value and finally got saturated when the exposure time exceeded 1 min. No significant decrease in sensitivity was observed even after an exposure >5 min. This would mean that surface poisoning due to longer exposure in LPG is minimal in these films.

3.4. FTIR and Raman studies

FTIR and Raman studies were performed at room temperature on the as-deposited SnO₂ films and rapid thermally annealed SnO₂/Pd composite films before and after exposure to LPG. The above studies would reflect the bonding environment in these films which may lead to a clearer understanding of the sensing mechanism (discussed later). Figs. 10 and 11 shows the FTIR and Raman spectra

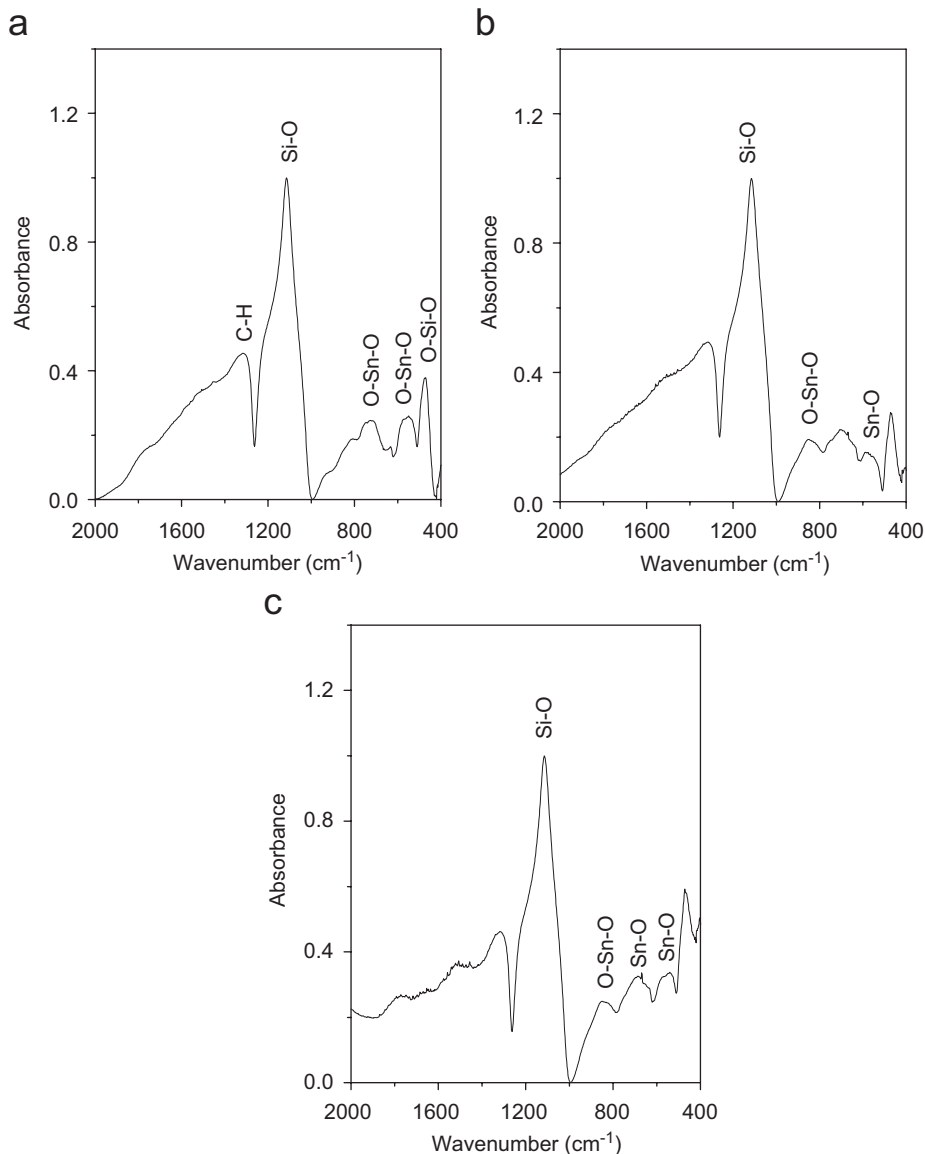


Fig. 10. FTIR spectra for: (a) as-deposited SnO₂ film; (b) Pd/SnO₂ film after RTP at 573 K for 5 min and (c) the same film as (b) but after LPG exposure.

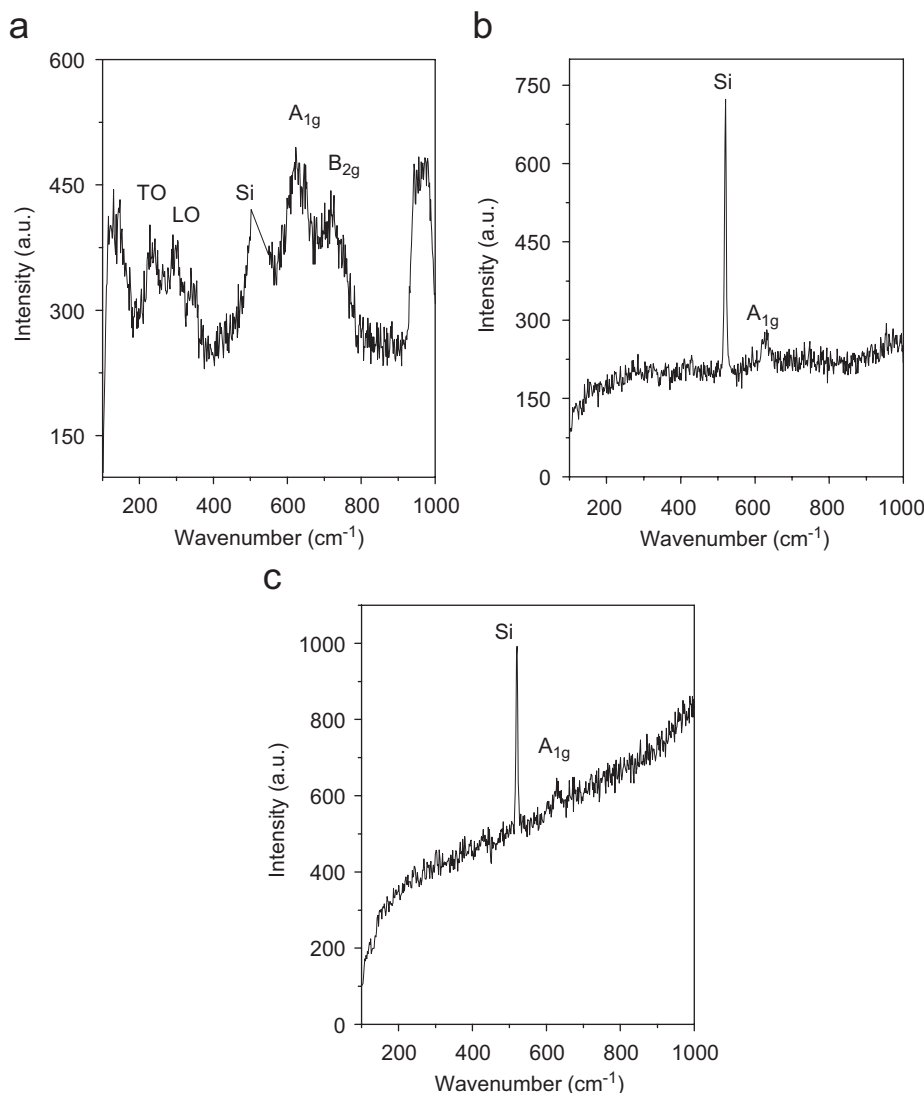


Fig. 11. Raman spectra for: (a) as-deposited SnO_2 film; (b) Pd/SnO_2 film after RTP at 573 K for 5 min and (c) the same film as (b) but after LPG exposure.

of the above films, respectively. It may be observed (Fig. 10(a)) that as-deposited SnO_2 films show the characteristic FTIR absorption due to Sn–O vibrational modes and O–Sn–O stretching modes at 549 and at $\sim 727\text{ cm}^{-1}$, respectively, along with peaks for O–Si–O, Si, Si–O and C–H at ~ 470 , 1114, 1180 and 1314 cm^{-1} , respectively, arising out of substrate and contamination from back-streaming of oil vapour of the pumping system. It may be noted here that the peak for Si at $\sim 1114\text{ cm}^{-1}$ appeared as a hump to the intense peak for Si–O at $\sim 1180\text{ cm}^{-1}$. There is a small hump at $\sim 850\text{ cm}^{-1}$ which may be ascribed to stretching modes for O–Sn–O. When this film with an over-layer of Pd was subjected to RTA, one may observe (Fig. 10(b)) that the small absorption peak for O–Sn–O stretching modes at $\sim 727\text{ cm}^{-1}$ disappeared and the stretching modes for O–Sn–O at $\sim 849\text{ cm}^{-1}$ became stronger. Additional small peak for Sn–O vibration bond appeared at $\sim 699\text{ cm}^{-1}$. The other peaks appearing

due to O–Si–O, Si, Si–O and C–H bonds remain invariant. Upon exposure to LPG, the peaks for Sn–O at ~ 549 and $\sim 727\text{ cm}^{-1}$ became prominent (Fig. 10(c)) and the peak due to stretching modes for O–Sn–O became less intense. This is possibly due to the presence of increased amount of oxygen vacant sites due to exposure to LPG culminating in an increase in electrical conductivity.

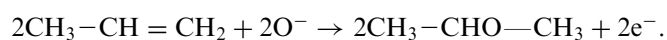
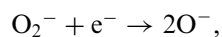
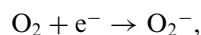
Raman spectra of the corresponding films are shown in Fig. 11. The spectrum for as-deposited SnO_2 film indicated (Fig. 11(a)) peaks at ~ 620 and 720 cm^{-1} for Raman active non-degenerate A_{1g} and B_{2g} modes. There are two additional peaks at ~ 220 and 300 cm^{-1} which are due to TO and LO acoustic phonon modes, respectively. A strong peak arising due to Si and originating from the substrate could be seen at $\sim 520\text{ cm}^{-1}$. Upon RTP with Pd overlayer on the top of SnO_2 , one may observe (Fig. 11(b)) that the peaks for LO and TO acoustic phonon modes became weaker and the peak for B_{2g} mode became weaker. When

the above film was exposed to LPG, the peak for the Raman active non-degenerate A_{1g} only was present (Fig. 11(c)). This may be due to the decrease in O–Sn–O bonds after the exposure to LPG.

3.5. Mechanism of LPG detection

LPG is generally a mixture of petroleum and other natural gases that exist in a liquid state at ambient temperature and moderate pressure. The main constituent of LPG is propane (~85% by liquid volume), butane (~2.5% by liquid volume) and propene (~5% by liquid volume). Among these constituents, propane and butane are more stable than propene which is an unsymmetrical alkene containing a double bond. Thus, propene is more prone to hydrogenation especially in the presence of catalysts like Pd and Ni. Additionally, propene is more reactive than alkanes as the π electrons of a double bond are located much further from the carbon nuclei and are less firmly bonded to them. Also the overlapping of the atomic orbitals in forming π bond is not as effective as that in σ bonds. Thus, the π bonds are weaker than the σ bonds and more easily broken.

Resistance of tin oxide films depends mainly on various oxygen-deficient sites present after deposition as well as on the doping level. Palladium was found to reside on the grains and at the grain boundaries of SnO_2 films. Presence of Pd in the film generates surface states and provides excess electrons to them. When such a film is heated at higher temperature, oxygen is adsorbed by the tin oxide layer and abstracts electron from the surface states thereby increasing the film resistance. This results in the formation of ionic species such as O^{2-} , O_2^- and O^- . Desorption of these oxygen species at the surface due to the possible hydrogenation form propene due to the presence of Pd and transport of electrons due to the breaking of π bonds of propane would culminate in an increase in conductance of the SnO_2 layer significantly in the presence of the sensing gas (LPG). Additionally, an increase in conductivity is also due to the reduction of the electronic potential barrier in the grain boundary of SnO_2 when oxygen is adsorbed on its surface. The adsorption/desorption of oxygen causes a change in Fermi level of the grains and hence changes the grain boundary potential barrier [20,21]. The reactions at the surface of films would be as follows:



At this juncture, it would be interesting to study the sensitivity of other gases like methane, hydrogen, ethanol and carbon dioxide and study the selectivity of the films. The films were exposed to methane, hydrogen, ethanol and carbon dioxide and experiments were performed as had been adopted for studying the sensitivity of Pd/ SnO_2 films

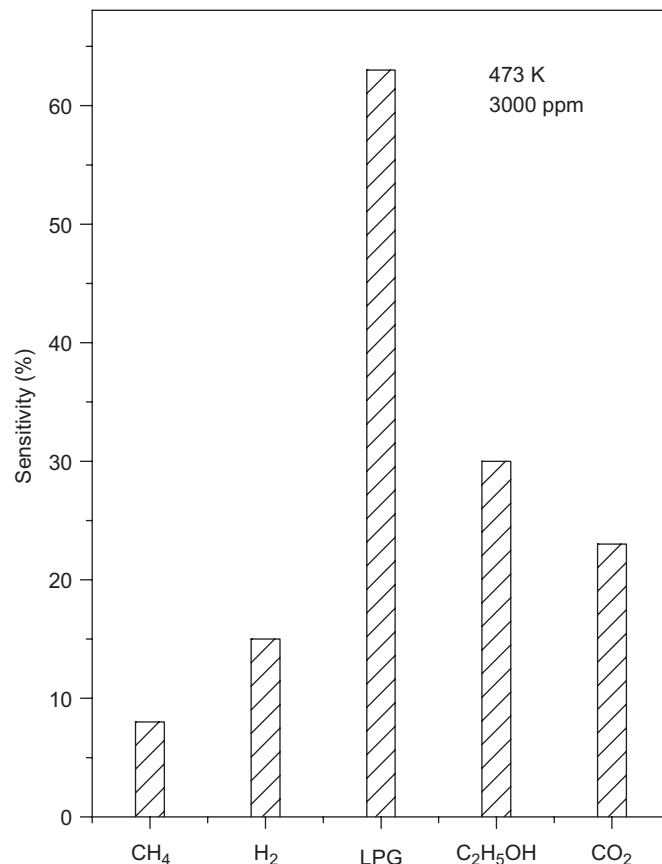


Fig. 12. Selectivity of a representative Pd/ SnO_2 film deposited on Si/ SiO_2 substrate.

used for LPG. The results are depicted in Fig. 12. The sensitivity for methane was found to be the lowest (~8%) followed by hydrogen (~15%), CO_2 (~23%) and $\text{C}_2\text{H}_5\text{OH}$ (30%). It could be asserted from this study that the selectivity for LPG was extremely good.

4. Conclusion

Pd/ SnO_2 bilayer films were obtained by DC sputtering of SnO_2 in argon plasma and evaporating a thin layer of Pd on it by vacuum evaporation. This Pd/ SnO_2 bilayer structure was subjected to rapid thermal annealing to disperse the Pd homogeneously in SnO_2 . XRD confirmed the presence of crystalline SnO_2 and Pd in these polycrystalline films. These films showed good LPG sensing property. The mechanism of sensing LPG was supposed to be based on the fact that propene was more prone to hydrogenation at higher temperatures and presence of catalyst like Pd might induce catalytic activity even at room temperature. Also, cracking of propane, the main constituent of LPG, to propene might also be possible at lower temperatures due to the presence of Pd leading to further hydrogenation activity in the films. Both the phenomena would culminate in an increase in conductivity of the SnO_2 /Pd films when exposed to LPG at increasing temperature. Sensitivity of 72% could be obtained at an operating

temperature of 573 K. The response time for these sensors was found to be ~ 27 s. Sensitivity was found to increase with grain growth at higher sensing temperatures. It could be observed that the selectivity for LPG was found to be extremely good as compared to the other gases like methane, hydrogen, CO₂ and C₂H₅OH.

Acknowledgments

One of the authors (SH) wishes to thank the Department of Science and Technology, Government of India, for extending a fellowship to her. Thanks are also due to Bharat Electronics Limited, Bangalore, India for supplying us with SiO₂-coated Si substrates.

References

- [1] Kohl DJ. *Phys D: Appl Phys* 2001;34:R125–49.
- [2] Katsarakis N, Bender M, Cimalla V, Gagaoudakis E, Kiriakidis G. *Sensors Actuators B* 2003;96:76–81.
- [3] Nanto HH, Sokooshi H, Usuda T. *Sensors Actuators* 1993;B10:79–83.
- [4] Hawk RM, Narayanaswamy A. *J Vac Sci Technol A* 1995;13:996–1000.
- [5] Nomura K, Shiozawa H, Takada T, Reuter H, Richter E. *J Mater Sci* 1997;8:301–8.
- [6] Lee DS, Kim YT, Hoo JS, Lee DD. *Thin Solid Films* 2002;416:271–8.
- [7] Fort A, Gregorkiewicz M, Machetti N, Rocci S, Serrano B, Tondi L, et al. *Thin Solid Films* 2002;418:2–8.
- [8] Ionescu R, Vansu A, Tomescu A. *Sensors Actuators B* 2000;69:283–6.
- [9] Sundaram KB, Bhagavat GK. *J Phys D: Appl Phys* 1981;14:333–8.
- [10] Poirier GE, Cavicchi RE, Semancik S. *J Vac Sci Technol A* 1993;11:1392–5.
- [11] Salehi A. *Thin Solid Films* 1998;324:214–8.
- [12] Mo Y, Okawa Y, Nakai T, Tajima M, Natukawa K. *Thin Solid Films* 2002;416:248–53.
- [13] Gordillo G, Moreno LC, Dela Cruz W, Teheran P. *Thin Solid Films* 1994;252:61–6.
- [14] Pan O, Xu J, Dong X, Zhang J. *Sensors Actuators B* 2000;66:237–9.
- [15] Manificiar JC, de Murcia M, Fillard JP, Vicario E. *Thin Solid Films* 1977;41:127.
- [16] Bhattacharyya D, Chaudhuri S, Pal AK. *Vacuum* 1992;4:313–6.
- [17] Pankove JI. In *Optical properties of semiconductors*. Englewood Cliffs, NJ: Prentice-Hall Inc; 1972.
- [18] Moss TS. *Optical Properties of Semiconductors*. London: Butterworths Scientific Publications; 1959. p. 34.
- [19] Korotcenkov G, Brinzari V, Boris Y, Ivanov M, Schwank J, Morante J. *Thin Solid Films* 2003;436:119–26.
- [20] Ihokura H, Okino K. *Sensor Technol* 1983;3:68–75.
- [21] Morrison SR. *Sensors Actuators* 1987;12:425–40.